Polymer Bulletin 43, 409–416 (1999)

Polymer Bulletin

Deposition of high fluorine content macromolecular thin layers under continuous-flow-system corona discharge conditions

S.-D. Lee, S. Manolache, M. Sarmadi*, F. Denes

Center for Plasma-Aided Manufacturing, and SHUEC, University of Wisconsin - Madison, Madison, WI 53706, USA

Received: 1 June 1999/Revised version: 1 September 1999/Accepted: 1 September 1999

Summary

High fluorine content macromolecular layers were deposited on polyethylene (PE) film surfaces under an originally designed, continuos-flow-system plasma reactor conditions. Survey and angle resolution, ESCA data and ATR-FTIR results indicate that the plasma-created films are thin and have a fairly uniform structure. The fluorinated layers have a 60% relative fluorine atomic concentration, and are mainly composed of CF_2-CF, and C-CF_3 groups. AFM images collected from virgin and plasma-exposed PE surfaces show a significantly rougher surface of the plasma-treated substrates. Applications can be envisaged for creating Teflon-like coatings on various polymeric film surfaces using a continuous plasma process.

Introduction

The fluorination of natural and synthetic polymeric substrates is a process of great importance, since it can provide special surface properties at an economical price, such as: chemical inertness, low dielectric constant, hydrophobicity, thermal stability, low friction, low electrical conductivity, low gas permeability, etc. Literature data indicate that plasma enhanced surface fluorination reactions can be carried out on even the most inert polymeric surfaces, both from saturated and unsaturated fluorocarbon compounds and their mixtures with oxygen, and from inorganic fluorides, by depositing macromolecular layers or by generating fluorine- and carbon-atom based functionalities (1-12). It was shown that the efficiencies of the deposition of fluorinated macromolecular layers depend strongly on the overall active fluorine-to-carbon ratio of the reaction mixture (13-20). Low fluorine-to-carbon ratios result in fluorinated plasma-"polymer" deposition processes, while high fluorine-to-carbon ratios lead to ablation (etching) reactions. CF_4-plasmas, for instance, do not deposit under common low density cold-plasma conditions macromolecular layers regardless of the nature of the substrates, in comparison to the volatile $(CF_2)_x$ (x = 1-4), and $C_xF_yX_z$ (X = H, Cl, Br, etc.) compounds where plasma films are instantaneously formed. However, it has been demonstrated that high density plasma conditions can lead to the deposition of fluorinated macromolecular layers even involving carbon tetrafluoride (21).

* Corresponding author

These plasmas usually require relatively low pressure environments (10-500 mT) and as a consequence batch-type installations are required in the deposition processes which considerably limit the application possibilities.

In this contribution the deposition of fluorinated macromolecular layers on polyethylene (PE) film rolls are described by using an originally designed, pilot scale, continuous-flow system, variable pressure plasma reactor.

Experimental

Materials and Methods

Additive free PE films (27 cm wide) were used in all experiments. ESCA data indicated that the PE substrates have a 0.4 % processing origin oxygen content. Carbon tetrafluoride was purchased from Matheson, and high purity argon from Liquid Carbonic.

Survey and high resolution X-ray photoelectron spectroscopy (ESCA) estimations were performed using a ESCA, Perkin Elmer Physical Electronics 0 5400 Small Area System (Mg source; 15 kV; 300 W; pass energy: 89.45 eV; angle: 15, 30, 45, 60 and 90 degrees.). Comparative relative surface atomic compositions (C1s, F1s, and O1s) from virgin and plasma treated samples were evaluated and the non-equivalent binding energy values of carbon were analyzed. Surface charge-origin binding energy shifts were also corrected relative to C1s C-C (285 eV) binding energy value. All high resolution ESCA binding energy assignments were performed according to SCIENTA ESCA 300 Database.

The presence of CF_x functionalities on the CF_4/Ar-plasma exposed PE surfaces has been evaluated by differential Attenuated Total Reflectance-Fourier Transform Infrared Spectroscopy (ATR-FTIR). An ATI-Mattson, Research Series IR instrument was used which was provided with a GRASEBY-Special Benchmark Series ATR in-compartment P/N/ 11160 unit. All FTIR evaluations were performed under nitrogen blanket generated from a flow-controlled liquid nitrogen tank. Data were collected in the 400-4000 cm^{-1} wavenumber region with 250 scans for each sample, and the high resolution-mode 800-1600 cm^{-1} wavenumber regions were compared. The differential spectra resulted from the substraction of reference spectra (ATR spectra of PE) from the ATR spectra of plasma-treated polymers.

The modified surface morphologies (deposition/etching) of plasma treated samples in comparison to virgin substrates were evaluated by atomic-force microscopy (Digital Instrument Nanoscopy III AFM; experimental conditions: wet cell (for avoiding surface charging effects); scan rate- 2.654 Hz, sampling number-512).

Plasma Treatments

All plasma treatments of PE films were performed using an original continuous-flow-system, reactive - gas, corona installation (RGC), (Figure 1), described earlier (22). The RGC reactor is composed of a variable pressure reaction chamber, a power supply, a vapor- and gas-feeding system (monomer and gas reservoirs, flow controllers, valves), and a vacuum installation (mechanical vacuum pump, valves, liquid nitrogen trap, and *in-situ* and *ex-situ* connecting lines). The elliptical cross-section, stainless steel reaction chamber, locates the freely rotating, hollow, stainless steel, grounded, central-electrode-roller (4), four linear electrodes (3) - housed in ceramic tubings, and embedded into a semicylindrical Teflon support (13), and the driving-rollers support (10). What is totally unique with this design is that the driving-roller assembly (6 and 7) - three out of four rollers - is located outside of the reaction chamber, and only half of one of the rollers has an *in-situ* position. This configuration

has a significant importance for practical applications; the rollers being not exposed to the plasma environment the usually difficult cleaning operations, related to polymer depositions, can significantly be reduced. It should be mentioned that the substrate admission and take-up rollers are located outside of the reaction chamber which allow a continuous-flow-system operation.

This plasma reactor allow the surface modification of bi-dimensional (films, fabrics, webs) natural and synthetic polymeric substrates (8) under the following experimental parameter range: Power dissipated to the electrodes: 0-500 W; Frequency of the driving field: 10 kHz; Voltage: 10 kV; Pressure range: 20 Torr-760 Torr; Speed of the substrate: 1-50 m/min.

In a typical experiment the following experimental conditions have been employed: Power 100 and 500 W; Pressure: 700 Torr; Plasma gas CF_4/Ar; Flow rates: CF_4: 7840 sccm, Ar: 11360 sccm; Speed of the PE substrate: 1m/min.

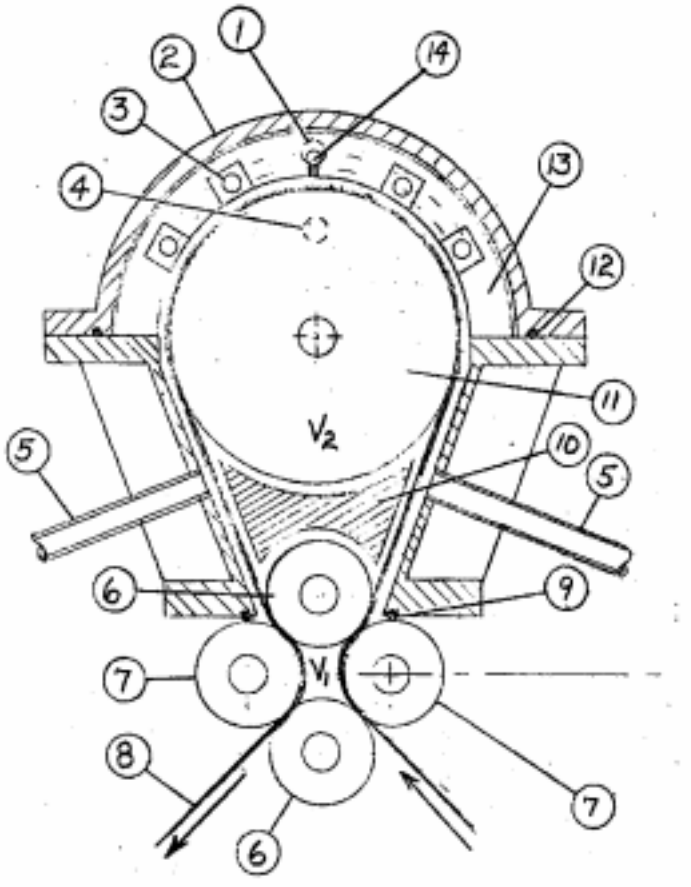

Figure 1. Schematic diagram of the continuous-flow-system, variable pressure plasma reaction chamber. 1-high voltage lead; 2-vacuum housing; 3-electrode; 4-ground contact; 5-vacuum line; 6-teflon covered hard roller; 7-teflon covered soft roller; 8-film; 9-seal rod; 10-roller support; 11-ground roller; 12-seal; 13-teflon electrode holder; 14-gas inlet; 15-face seal surface; 16-ball bearing assembly.

Results and discussion

Survey ESCA data indicate that carbon and fluorine atoms are the main components of the plasma exposed surface layers (Figure 2), and that relative surface fluorine atomic concentrations close to 60% can be achieved under high CF_4 content CF_4/Ar-plasma environments. It also should be observed that higher power values (e.g. 400 W) generate surface layers with only slightly higher fluorine concentrations and lower oxygen contents (Table I). This might be explained by the presence of an intense functionalization / deposition mechanism, and by the short residence time of the substrate in the plasma zone.

Table I. Effect of power on the surface fluorine concentration

Power (W)	*C (%)*	*O (%)*	*F (%)*
100	39.14	3.02	57.84
400	37.50	2.58	59.92

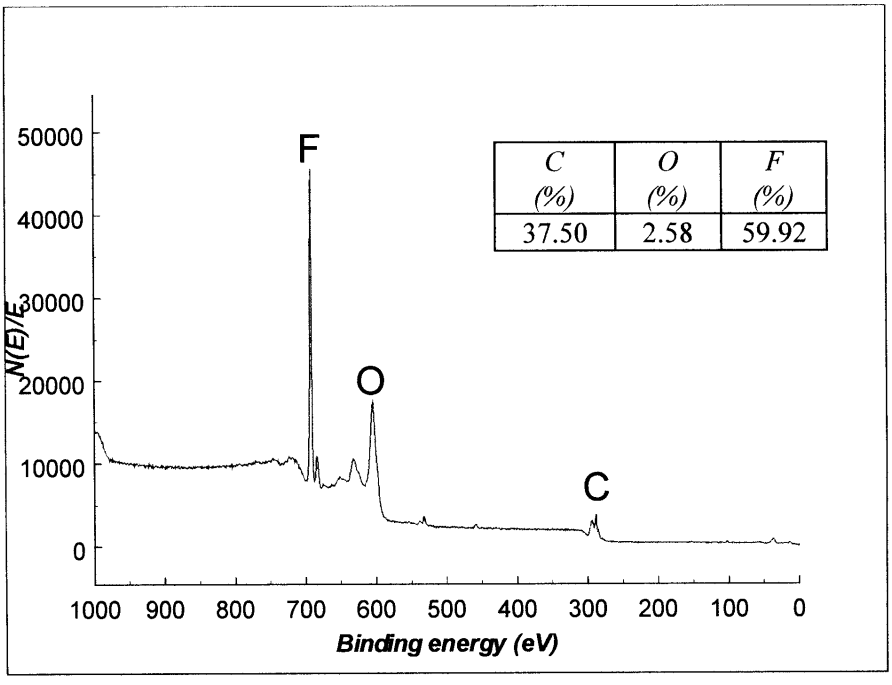

C (%)	O (%)	F (%)
37.50	2.58	59.92

Figure 2. Survey ESCA diagram and relative surface atomic concentration of CF_4/Ar- plasma treated PE substrate (Power: 400 W; Pressure: 700 T; Relative CF_4/Ar flow rates: 7840 / 11360 sccm; Speed of the substrate: 1 m/min).

High resolution ESCA results indicate the presence of a complex CF_x-based (x<4) thin surface layer (Figure 3). Besides the characteristic, polyethylene origin, C-C, C-H binding energy peak (285 eV), fairly intense $^*CF_3$-CF (293.3 eV), $^*CF_2$-CF (291.5 eV), CF_3-*CF-CF_2 (289.3 eV), *CHF-CH_2 (287.9 eV), and $^*CF_2$-CH_2 (286.6) binding energy peaks can be identified. It should be mentioned that the area of the C-C binding energy peak represent only 37% of the total peak area.

Angle	C^*H_2-CH_2 285 eV	C^*F_2-CH_2 286.6 eV	C^*HF-CH_2 287.9 eV	CF_3-C^*F-CF_2 289.3 eV	C^*F_2-CF 291.5 eV	C^*F_3-CF 293.3 eV
45°	**38.4**	10.4	4.5	17.6	21.0	8.1

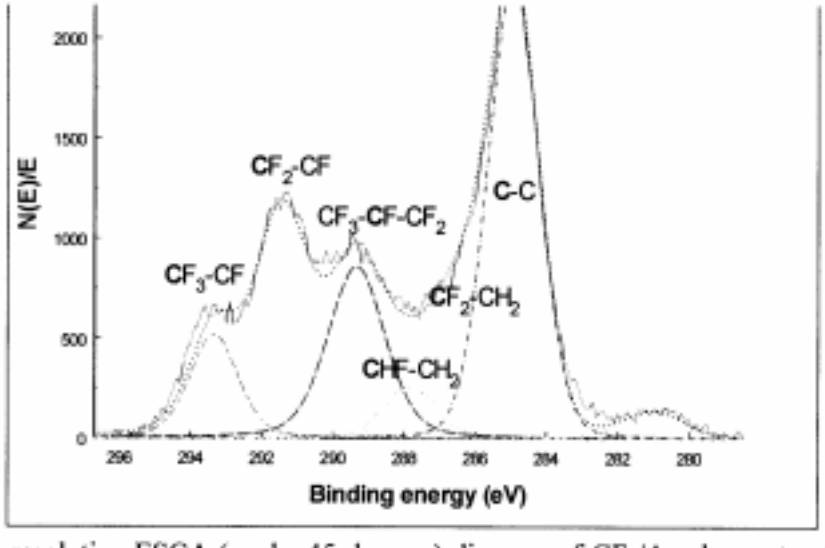

Figure 3. High resolution ESCA (angle: 45 degrees) diagram of CF_4/Ar-plasma treated PE (Power: 400 W; Pressure: 700 Torr; Relative CF_4/Ar flow rates: 7840/11360 sccm; Speed of the substrate: 1 m/min), and the relative surface areas of the non-equivalent C1s binding energy functionalities.

In order to learn more about the thickness and structural uniformity of the fluorinated layers, angular resolution ESCA analyses were performed (Figure 4 and Table II).

Table II. Angular resolution ESCA data of the ratios of non-equivalent C1s functionalities

Angle	*C*H$_2$-CH$_2$ 285 eV*	*C*F$_2$-CH$_2$ 286.6 eV*	*C*HF-CH$_2$ 287.9 eV*	*CF$_3$-C*F-CF$_2$ 289.3 eV*	*C*F$_2$-CF 291.5 eV*	*C*F$_3$-CF 293.3 eV*
90°	**47.2**	8.4	4.5	14.5	16.7	8.7
60°	**42.7**	9.4	4.9	15.2	17.9	8.9
45°	**38.4**	10.4	4.5	17.6	21.0	8.1
30°	**34.3**	7.6	5.3	19.2	23.2	10.4
15°	**29.3**	7.5	6.4	19.8	25.2	11.8

One can notice that the relative ratios of CF_x peak surface areas do not change significantly with the selected angle (depth of the acquisition) and that the total surface area of the CF_x peaks increases deramatically as the angle is decreasing, while the area of C-C peak

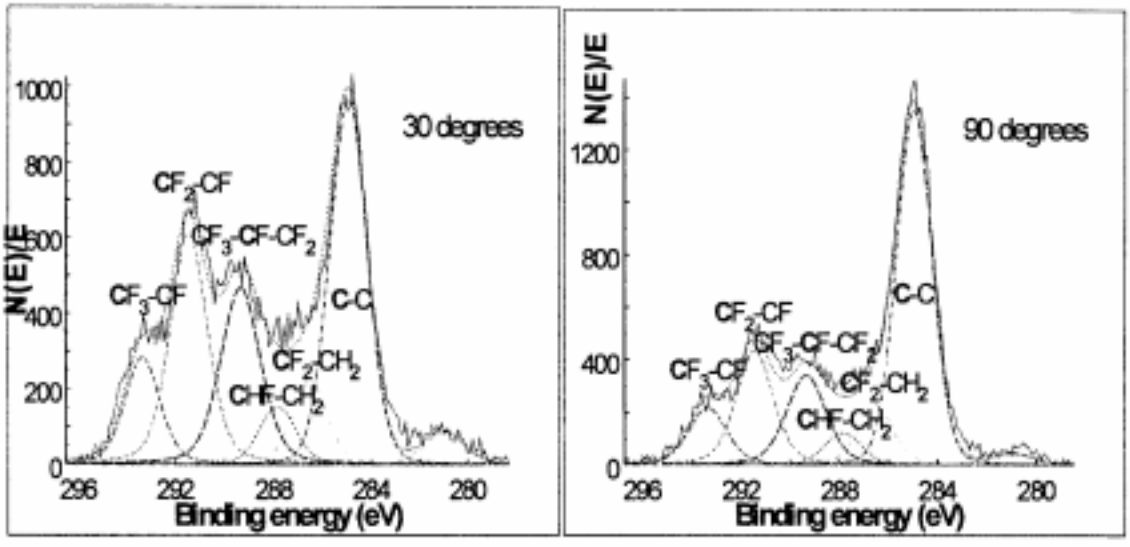

Figure 4. Comparative high resolution angular resolution ESCA diagrams of CF_4/Ar-plasma treated PE (Power: 400 W; Pressure: 700 Torr; Relative CF_4/Ar flow rates: 7840 / 11360 sccm; Speed of the substrate: 1 m/min).

followes an opposite behavior. This clearly indicate the presence of a very thin (< 100Å thickness) and fairly uniform-structure fluorinated layer. At lower angles the ESCA diagrams evidence the fluorinated top-layer structure, while higher angles exhibit gradually a more PE-like material. Relative surface atomic composition resulting from angular resolution ESCA data (Table III) reflect the same pattern. More hydrocarbon-like structures can be identified in the deeper PE layers.

Table III. Angular resolution ESCA data of relative surface atomic concentration

Angle between detector and sample	*C (%)*	*O (%)*	*F (%)*
90°	39.46	2.63	57.91
60°	38.76	2.27	58.97
45°	37.50	2.58	59.92
30°	36.45	2.74	60.81
15°	35.67	2.13	62.20

Experiments run under stationary substrate conditions and at various plasma-exposure intervals (Table IV) show similar relative atomic composition values. This indicate that treatment times as low as 1 min are enough for depositing a high fluorine content surface layer.

The 10 KHz, DC power has a significant effect on the relative ratios of non-equivalent C1s functionalities (Table V). Higher powers generate lower C-C and C-H bond involvement and higher CF_x concentrations. An efficient deposition of perfluorinated network layers, as a result of a more intense molecular fragmentation of CF_4, is suggested to be responsible for this phenomenon.

The formation of a very thin perfluorinated macromolecular layer on the PE surfaces is also evidenced by Differential ATR-FTIR spectroscopy (Table VI). The IR spectrum resulting from the subtraction of the spectrum of virgin PE from the spectrum of CF_4/Ar-plasma-treated PE clearly indicate the presence of CF_2 (1245 cm^{-1}), CF_3 (1376 cm^{-1}) and CF (1079 cm^{-1}) absorptions, and which are totally absent in the spectrum of untreated PE. The relative ratio of CF_x / CH_2 peak areas also show that higher CF_x functionality concentrations are associated with higher RF power values.

Table IV. ESCA data for stationary-substrate conditions at various plasma-exposure intervals (CF_4 and Ar, 700 mTorrs)

Time (min)	*C (%)*	*O (%)*	*F (%)*
1	32.26	0.79	66.95
2	33.24	0.72	66.04
3	32.92	0.75	66.33

Table V. Effect of power on the relative ratios of non-equivalent C1s functionalities.

Power (W)	*C*H₂-CH₂ 285 eV*	*C*F₂-CH₂ 286.6 eV*	*C*HF-CH₂ 287.9 eV*	*CF₃-C*F-CF₂ 289.3 eV*	*C*F₂-CF 291.5 eV*	*C*F₃-CF 293.3 eV*
100 W	44.7	11.9	8.7	12.5	8.8	13.4
400 W	38.3	10.4	4.5	17.6	21.1	8.1

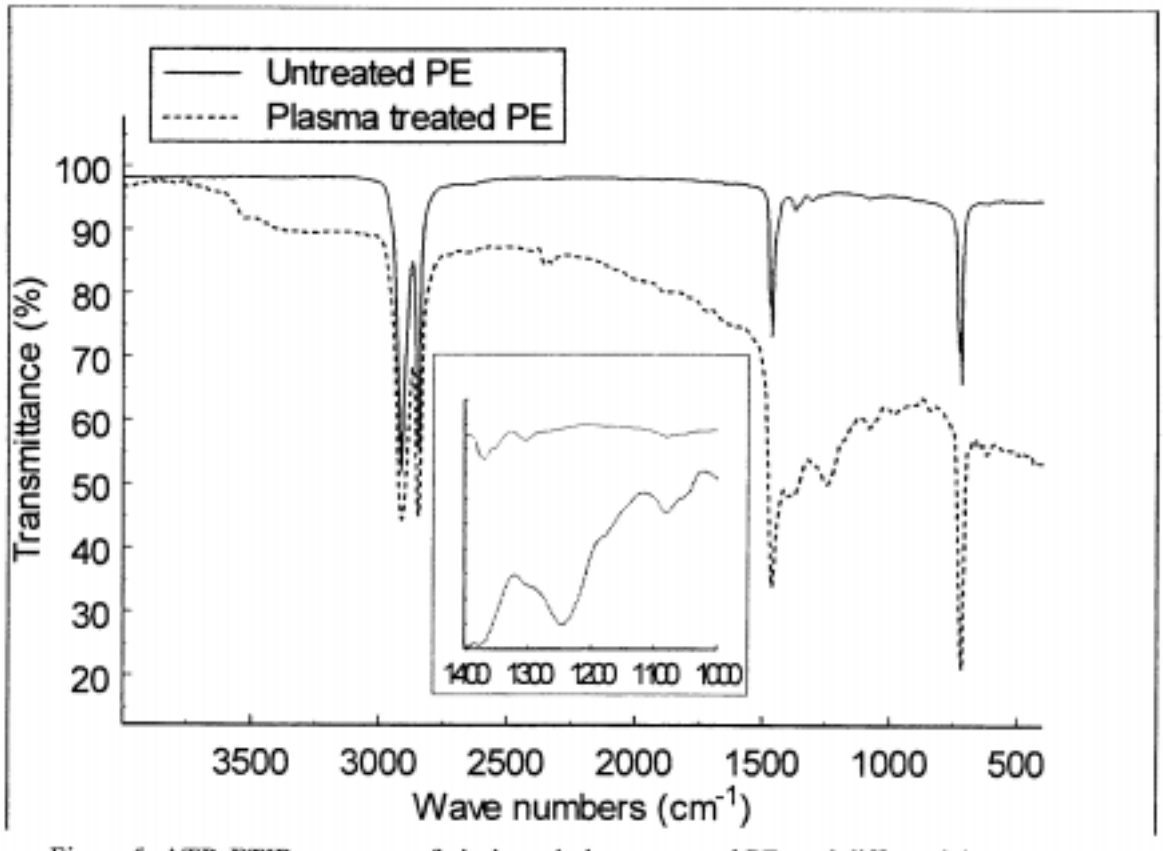

Figure 5. ATR-FTIR spectrum of virgin and plasma-treated PE, and differential ATR-FTIR spectrum of CF_4/Ar-plasma treated PE in the 800-1500 cm^{-1} wavenumber range.

Table VI. Ratio of CF_x to CH_2 peak areas derived from ATR-FTIR spectra (CF_4 and Ar, 700 mTorrs)

Power (W)	*CH_2 area (1529-1411)*	*CF_x area (1328-954)*	*Ratio CF_x/CH_2*
100	1002	226	0.23
250	1088	397	0.36
400	1055	423	0.40

AFM images of virgin and plasma-modified PE surfaces (Figure 6) show that a more intense surface roughness is associated with the plasma-treated substrates. RMS values as high as 15 characterize the plasma-exposed PE while the virgin substrates exhibit only RMS values around 4. This allow us to suggest that the deposition of fluorinated macromolecular layers are accompanied by an intense etching mechanism. This is not surprising due to the presence of fluorine atoms in the discharge as a result of molecular fragmentation.

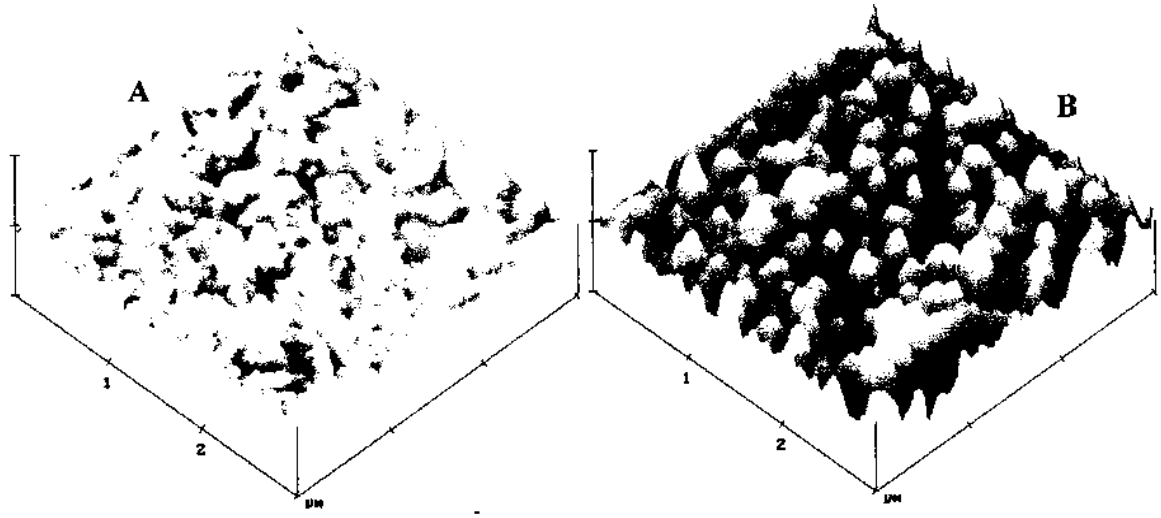

Figure 6. AFM images of virgin (A) and CF_4/Ar-plasma treated (B) PE.

Comparative water-contact-angle data (Table VII) resulting from polyethylene and CF_4-plasma-treated PE surfaces indicate stable, improved hydrophobicity of plasma-exposed substrate surfaces.

Table VII. Time-dependent contact angle values for PE and CF_4-plasma-treated PE

Power (W)	*Water-contact-angle values (degree)*	
	After 1 hour	*After 100 days*
Untreated	96	96
100	110	111
250	115	115
400	115	113

Conclusions

RGC, CF_4/Ar-plasma conditions are proper for the deposition of very thin perfluorinated macromolecular layers on PE surfaces. The deposition reactions are accompanied by intense etching mechanisms. Potential applications of this technology for the creation of very thin Teflon-like layers in a continuous manner, on various films surfaces are envisaged.

References

1. Anand M., Cohen R.E., and Baddour R.F., Polymer, vol.22, March, p. 361, (1981).
2. Astell-Burt P.J., Cairns J.A., Cheetham A.K., and Hazel R.M., Journal of Plasma Chemistry and Plasma processing, vol.6, no. 4, p. 417, (1986).
3. Dedinas J., Feldman M.M., Mason M.G., and Gerenser L.J., Paper presented at the First International Conference of Plasma Research and Technology, San Diego, CA, Nov. 14-17, p. 119, (1982).
4. Momose Y., Takada T., and Okazaki S., Proc., ACS Div. Polym. Mat. Sci. Eng., 56, p. 236, (1987).
5. Arefi F., Montazer-Rahmati P., Andre V., and Amoroux J., J. Appl. Polym. Sci: Applied Polymer Symposium, 46, p. 33, (1990).
6. Denes F., Sarmadi A.M., C.E.C.A. Hop, M. Buncick, and R.A. Young, J. Appl. Polym. Sci., vol.52, p. 1419, (1994).
7. Liston E.M., Martinu L., and Wertheimer R., J. Adhesion Sci. Technol., vol.10, p.1091, (1993).
8. Plumb I.C., and Ryan K.R., Plasma Chemistry and Plasma processing, vol.6, no.3, p.205, (1986).
9. Yagi T., and Pavlath A.E., J. Appl. Polym, Sci.: Applied Polymer Symposium, 38, p. 215, (1984).
10. Millard M.M., Windle J.J., and Pavlath A.E., J. Appl. Polym. Sci., vol.17, p. 2501, (1973).
11. Yagi T., Pavlath A.E., and Pittman A.G., J. Appl. Polym. Sci., vol.27, p., (1982).
12. Yagi T., Pavlath A.E., and Pittman A.G., Proc. of V. International Symposium on Plasma Chemistry, Edinburg, Scotland, Sept., (1981).
13. Winters H.F., Coburn J.W., and Kay E., J. Appl. Phys., 48, p. 4973, (1977).
14. Kay E., Dilks A., and Seybold D., J. Appl. Phys., 51, p. 4973, (1977).
15. Kay E., Coburn J.W., and Dilks A., Top. Curr. Chem., 94, p. 1; Plasma Chemistry, vol. III, Springer, Berlin, (1980).
16. Kay E., and Dilks A., Thin Solid Films, 78, p. 309, (1981).
17. Klausner M., Baddour R.F., and Cohen R.E., Polymer Engineerig and Science, June, vol. 27, no. 11, p. 861, (1987).
18. Montazer Rahmati P., Arefi F., and Amoroux J., Surface and Coatings Technology, 45, p. 369, (1991).
19. Strobel M., Corn S., Lyons C. S., and Korba G.A., J. Polym. Sci.: Polymer Chemistry Edition, vol. 23, p. 1125, (1985).
20. d'Agostino R., de Benedictis D., and Cramarossa F., Plasma Chem. Plasma Process., 4(1), p.1, (1984).
21. Oehrlein G.S., Zhang Y., Vender D., and Haverlag. M., J. Vac. Sci. Technol. A 12 (2), p. 323, (1994).
22. S. D. Lee, S. Manolache, M. sarmadi and F. Denes, Hakone VI - International Symposium on High Pressure, Low Temperature Plasma Chemistry, P. 93-97, Cork, Ireland (1998).